Asian Journal of Control, Vol. 16, No. 2, pp. 335–344, March 2014
Published online 14 May 2013 in Wiley Online Library (wileyonlinelibrary.com) DOI: 10.1002/asjc.731

ADAPTIVE LIPSCHITZ OBSERVER DESIGN FOR A MAMMALIAN MODEL

Long Ton That and Zhengtao Ding

ABSTRACT

This paper deals with observer designs for a proposed mathematical model of circadian rhythms which exist in almost every living organism. A 7th order model for mammalian circadian rhythms which captures the main dynamic features is considered in this paper. A recent result of one-sided Lipschitz observer design in the literature is applied to this mammalian model to show a possibility of reducing measurements for circadian models in system biology. The mammalian model presented may contain an uncertainty parameter. An adaptive design of the Lipschitz observer is then applied to deal with this case. Besides detailed designs of both observers, detailed analysis is also performed for nonlinear functions in the mammalian model to show that the Lipschitz observers can indeed be applied. Several simulation studies of the proposed observers are carried out with the results shown in this paper.

Key Words: Biological systems, observers, state estimations, parameter estimation.

I. INTRODUCTION

Circadian rhythms exist as self-sustained, periodic oscillations, and govern the daily biological activities of almost every living species on Earth. Physiological functions such as sleep-wake cycle, blood pressure, and heart rate are examples of circadian rhythms. Robustness to external environmental changes is one of the typical properties of these rhythms. Circadian rhythms can be disrupted, and this phenomenon is known as circadian disorder. Jet lag and sleeping-disorder are two well known phenomena of circadian disorders. Lack of treatment of circadian disorders may lead to negative impact on daily activities and health.

Because of the importance of circadian rhythms for daily life, research study of characteristics of circadian rhythms has attracted the attention of researchers over many years. A lot of results have been achieved (for example, [1–3]). Among the results presented in the literature, the identification of key genes which contribute to oscillations of circadian rhythms [4–7] and the constructions of circadian models [8–11] are the most successful achievements. With the existence of the circadian models, different areas of research on circadian rhythms have been carried out, *e.g.* analyses of amplitude under light constraints [12], entrainment in light/dark cycle [13], robustness analysis [14], and sensitivity analysis [15,16].

Manuscript received April 2, 2012; revised November 21, 2012; accepted February 21, 2013.

Long Ton That (e-mail: Long.TonThat@postgrad.manchester.ac.uk) and Zhengtao Ding (corresponding author, e-mail: zhengtao.ding@manchester.ac.uk) are with Control System Center, School of Electrical and Electronic Engineering, The University of Manchester, Manchester M13 9PL, UK

Recently, a result has been reported on the application of a high gain observer design to Neurospora model [17]. In control theory, observers are designed to estimate the unknown state variables in both linear and nonlinear systems. Therefore, they are often used for control implementations when unmeasured state variables are needed, *e.g.* [18]. With only a few measurements, we can estimate all state variables of the systems considered. Therefore, using an observer also helps to reduce the number of output measurements.

Reducing measurements by using observers has not been much considered in system biology, especially for circadian models. This may be due to the advancements of technology, and the development of many experimental methods which make measurements of circadian rhythms easier and faster in practice. It may be also due to a lack of the right methods for observer designs in the past. Nevertheless, in recent years, some new methods of observer design have been developed, such as reduced order observer [19], and Lipschitz observer design [20]. An observer is called a Lipschitz observer if its design is based on systems with Lipschitz nonlinearities. Since the mathematical model of mammalian circadian rhythms consists of nonlinear functions which are Lipschitz nonlinearities, Lipschitz observer design is suitable in this case. The application of Lipschitz observer design to circadian models has been presented in [28]. The Lipschitz observer design proposed in [28] is based on the result recently obtained in [20] for one-sided Lipschitz observers. In this paper, we review the application of this observer design to a mammalian model of circadian rhythms.

In theory, mathematical models of circadian rhythms are created based on developed hypotheses. Values of parameters involved in these mathematical models are chosen, and

© 2013 Chinese Automatic Control Society and Wiley Publishing Asia Pty Ltd

then adjusted to satisfy these hypotheses. Therefore, these values can be considered as uncertainties. With the involvement of uncertainty parameters, the Lipschitz observer design considered in [28] is inadequate. In the literature, there are a lack of suitable adaptive observer designs which can be applied to circadian models due to their complicated nonlinear functions. Given that the mathematical model of mammalian circadian rhythms may have unknown parameters, we also propose an adaptive Lipschitz observer design to the model in this paper. The proposed adaptive Lipschitz observer is based on the result obtained in [27].

II. MAMMALIAN MODEL

Circadian model of mammals is a 7th order model, and was proposed in [11] to investigate negative and positive feedback in a mammalian circadian oscillator. This model describes the molecular mechanism of mammalian circadian rhythms.

In mammals, the *Per2*, *Cry*, and *Bmal1* genes have been identified as part of circadian oscillations. The *Clock* gene has also been identified as part of circadian oscillations in mammals. The expression of the *Clock* gene, CLOCK protein, together with the expression of the *Bmal1* gene, BMAL1 protein, are phosphorylated to form a heterodimer which activates the transcriptions of *Per2* and *Cry* genes [11]. However, since the CLOCK protein is expressed at a constant level [21], only the oscillation of the BMAL1 protein is considered in the mechanism described in [11]. Furthermore, the heterodimer BMAL1/CLOCK which activates the transcriptions of *Per2* and *Cry* genes is now replaced by BMAL1*. BMAL1* is considered as a phosphorylated form of BMAL1 [11,22], or as a complex with CLOCK protein [11,23]. The mechanism starts with the activation of BMAL1* to the transcription of *Per2* to produce *Per2* mRNA, and the transcription of *Cry* genes to produce *Cry* mRNA. However, in this mechanism, the expressions of the *Per2* gene and *Cry* gene, which are mRNAs of *Per2* and *Cry*, and their proteins, are represented by the same variables [11].

Dynamics of the involved mRNAs and proteins are described by the following set of differential equations:

$$
\begin{aligned}
\dot{x}_1 &= \frac{v_{1b}(x_7+c)}{k_{1b}\left(1+\left(\frac{x_3}{k_{1i}}\right)^p\right)+x_7+c} - k_{1d}x_1\\
\dot{x}_2 &= k_{2b}x_1^q - (k_{2d}+k_{2t})x_2 + k_{3t}x_3\\
\dot{x}_3 &= k_{2t}x_2 - (k_{3t}+k_{3d})x_3\\
\dot{x}_4 &= \frac{v_{4b}x_3^r}{k_{4b}^r+x_3^r} - k_{4d}x_4,\\
\dot{x}_5 &= k_{5b}x_4 - (k_{5d}+k_{5t})x_5 + k_{6t}x_6\\
\dot{x}_6 &= k_{5t}x_5 - (k_{6t}+k_{6d}-k_{6a})x_6 + k_{7a}x_7\\
\dot{x}_7 &= k_{6a}x_6 - (k_7+k_{7d})x_7
\end{aligned}
\tag{1}
$$

where x_1, x_2, and x_3 represent concentrations of *Per2*/*Cry* mRNA, PER2/CRY complex protein in cytoplasm, and PER2/CRY complex in nucleus respectively. State x_4 denotes concentration of *Bmal1* mRNA. State x_5 denotes concentration of BMAL1 protein in cytoplasm, and state x_6 represents nuclear BMAL1 protein. State x_7 represents the concentration of BMAL1*. All of the state variables are assumed to be positive values. Default values of the parameters involved in (1) are given in [11] as $v_{1b}=9nM.h^{-1}$, $k_{1b}=1nM$, $k_{1i}=0.56nM$, $c=0.01nM$, $p=8$, $k_{1d}=0.12h^{-1}$, $k_{2b}=0.3nM^{-1}.h^{-1}$, $q=2$, $k_{2d}=0.05h^{-1}$, $k_{2t}=0.24h^{-1}$, $k_{3t}=0.02h^{-1}$, $k_{3d}=0.12h^{-1}$, $v_{4b}=3.6nM.h^{-1}$, $k_{4b}=2.16nM$, $r=3$, $k_{4d}=0.75h^{-1}$, $k_{5b}=0.24h^{-1}$, $k_{5d}=0.06h^{-1}$, $k_{5t}=0.45h^{-1}$, $k_{6t}=0.06h^{-1}$, $k_{6d}=0.12h^{-1}$, $k_{6a}=0.09h^{-1}$, $k_{7a}=0.003h^{-1}$, $k_{7d}=0.09h^{-1}$. The physical meanings of these values are also found in [11].

A simulation study has been carried out in MATLAB. The initial condition of (1) is chosen with $x(0)=[0.25\ \ 0.28\ \ 0.85\ \ 0.3\ \ 0.25\ \ 0.6\ \ 0.855]^T$. The dynamics of the state variables are shown in Fig. 1.

III. OBSERVER DESIGNS

In this section, two design procedures of Lipschitz and adaptive Lipschitz observers which are obtained in [20] and [27] are briefly summarized.

3.1 Lipschitz observer design

Consider a class of nonlinear system which is described by:

$$
\begin{aligned}
\dot{x} &= Ax + \varphi(x,u),\\
y &= Cx
\end{aligned}
\tag{2}
$$

where $x \in \mathbb{R}^n$ is the state vector, $u \in \mathbb{R}^p$ is the input, $y \in \mathbb{R}^m$ is the output, $\varphi(x,\ u) \in \mathbb{R}^n \times \mathbb{R}^m \to \mathbb{R}^n$ is nonlinear function,

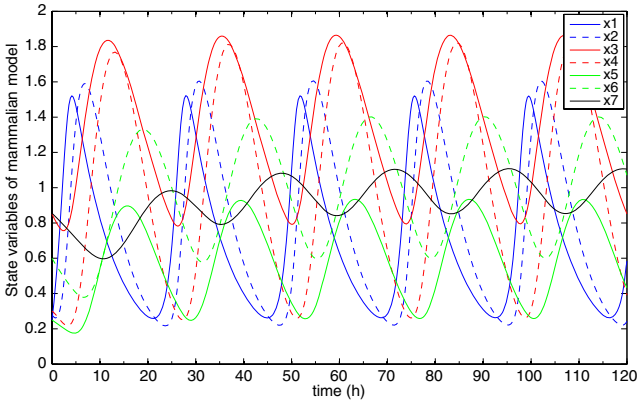

Fig. 1. Dynamics of state variables.

© 2013 Chinese Automatic Control Society and Wiley Publishing Asia Pty Ltd

$A \in \mathbb{R}^{n\times n}$ and $C \in \mathbb{R}^{m\times n}$ are constant matrices. If $\varphi(x, u)$ satisfies the Lipschitz condition described by

$$\|\varphi(x,u)-\varphi(\hat{x},u)\| \le \gamma \|x-\hat{x}\|, \forall x, \hat{x} \in \mathbb{R}^n, \tag{3}$$

where γ is the Lipschitz constant, $\varphi(x, u)$ is called the Lipschitz nonlinearity. Another condition is called the one-sided Lipschitz condition which is described by

$$\langle f(x,u)-f(\hat{x},u), x-\hat{x}\rangle \le \upsilon_p \|x-\hat{x}\|^2, \tag{4}$$

$\forall x, \hat{x} \in \mathbb{R}^n$, where υ_p, which may be a negative value, is one-sided Lipschitz constant. In addition, $f(x, u) = P\varphi(x, u)$, where P is a positive definite matrix, and <.,.> is a Euclidean product on $\mathbb{R}^n$. If $\varphi(x, u)$ satisfies (4), $\varphi(x, u)$ is called a one-sided Lipschitz nonlinearity.

For such nonlinear systems as (2), the observer can be designed as

$$\dot{\hat{x}} = A\hat{x} + \varphi(\hat{x},u) + L(y - C\hat{x}), \tag{5}$$

where L is the observer gain with $L \in \mathbb{R}^{n\times m}$. If $\varphi(x, u)$ satisfies (4), according to the result presented in [24], the value of L of the one-sided Lipschitz observer design (5) is given by a following theorem:

Theorem 1. If a gain L is chosen such that $(A - LC)$ is stable and the following inequality

$$(A-LC)^T P + P(A-LC) + 2\upsilon_p I < 0 \tag{6}$$

is satisfied, where P is a positive definite matrix, and υ_p is one-sided Lipschitz constant of $f(x, u) = P\varphi(x, u)$ such that (4) holds, the observer (5) yields asymptotically convergence estimate for system (2).

The condition for the existence of the observer gain L such that (6) admits a positive definite matrix solution P, and how to obtain value of this gain L, are not shown in [24]. This problem is solved by the new result of one-sided Lipschitz observer design shown in [20]. The new observer design is given through a theorem which is described below.

Theorem 2. Consider the nonlinear system (2) with condition (4). If there exists a positive value σ such that the following condition

$$A^T P + PA - \sigma C^T C + 2\upsilon_p I < 0 \tag{7}$$

is satisfied, where P is a positive definite matrix, and υ_p is one-sided Lipschitz constant. The observer (5) having $L = \frac{\sigma}{2} P^{-1} C^T$ as the observer gain yields an asymptotical convergence estimate for system (2).

Given that $\varphi(x, u)$ is Lipschitz nonlinearity, according to [20], instead of (7), linear matrix inequality (LMI) is modified with the form described by

$$A^T P + PA - \sigma C^T C + 2n\sum_{i=1}^{n} \gamma_i \lambda_i I < 0, \tag{8}$$

where γ_i indicates the Lipschitz constant for each Lipschitz nonlinear functions, n denotes number of state variables of the system, and λ_i is small positive real constant. Value of λ_i can be chosen such that $n\sum_{i=1}^{n} \gamma_i \lambda_i < \left(\sum_{i=1}^{n} \gamma_i^2\right)^{\frac{1}{2}}$.

3.2 Adaptive Lipschitz observer design

Consider a class of nonlinear system which is described by

$$\begin{aligned} \dot{x} &= Ax + b\varphi(x,u)\theta + \phi(x,u), \\ y &= Cx \end{aligned} \tag{9}$$

where $x \in \mathbb{R}^n$ is the state vector, $y \in \mathbb{R}^m$ is the output, $b \in \mathbb{R}^{n\times s}$, $\theta \in \mathbb{R}^p$, $\varphi(x, u) : \mathbb{R}^n \to \mathbb{R}^{s\times p}$ and $\phi(x, u) : \mathbb{R}^n \to \mathbb{R}^n$ are nonlinear functions, A and C are constant matrices with appropriate dimensions.

The nonlinear system (9) has the following conditions:

1. $\phi(x, u)$ is a Lipschitz nonlinearity which satisfies (3) and has γ_1 as its Lipschitz constant:

$$\|\phi(x,u)-\phi(\hat{x},u)\| \le \gamma_1 \|x-\hat{x}\| \tag{10}$$

2. $\varphi(x, u)$ is also a Lipschitz nonlinearity which satisfies (4) and has γ_2 as its Lipschitz constant:

$$\|\varphi(x,u)-\varphi(\hat{x},u)\| \le \gamma_2 \|x-\hat{x}\| \tag{11}$$

3. The unknown parameter θ is bounded

$$\|\theta\| \le \gamma_3 \tag{12}$$

4. There exists a positive definite P such that

$$b^T P = C_1 \tag{13}$$

where $C_1 \in$ span(rows of C)

Remark 1. Condition (4), $b^T P = C_1$, can be alternatively tested by $b^T P C^{\perp} = 0$, where $C^{\perp}$ is the orthogonal projection on to null(C). Detail of finding value of $C^{\perp}$ is given in [27].

For nonlinear system (9), the adaptive observer can be designed as

$$\dot{\hat{x}} = A\hat{x} + b\varphi(\hat{x},u)\hat{\theta} + \phi(\hat{x},u) + L(y - C\hat{x}) \tag{14}$$

© 2013 Chinese Automatic Control Society and Wiley Publishing Asia Pty Ltd

The adaptive control law is described by

$$\dot{\hat{\theta}} = \rho^{-1}\varphi(\hat{x}, u)^T b^T P e, \tag{15}$$

where $e = x - \hat{x}$ and $\rho > 0$ is the adaptive gain. The value of the observer gain L in (14) can be found in the following theorem.

Theorem 3. Consider the nonlinear system (9) with conditions (1) to (4). If there exists a positive value σ such that

$$A^T P + PA - \sigma C^T C + (\gamma_1 + \gamma_2\gamma_3\|b\|)PP + (\gamma_1 + \gamma_2\gamma_3)I < 0 \tag{16}$$

is satisfied, the adaptive observer (14) with adaptive law (15) which has $L = \frac{\sigma}{2}P^{-1}C^T$ as its observer gain value yields asymptotically convergence estimate for system (9).

Proof. From $L = \frac{\sigma}{2}P^{-1}C^T$, we obtain $PL = \frac{\sigma}{2}C^T$. A substitution of $\frac{\sigma}{2}C^T = PL$ in to inequality (16) obtains a new LMI which is described by

$$\begin{aligned} &A^T P + PA - PLC - PLC + (\gamma_1 + \gamma_2\gamma_3)I \\ &\quad + (\gamma_1 + \gamma_2\gamma_3\|b\|)PP < 0 \leftrightarrow A^T P + PA - PLC - C^T L^T P \\ &\quad + (\gamma_1 + \gamma_2\gamma_3)I + (\gamma_1 + \gamma_2\gamma_3\|b\|)PP < 0 \\ &\quad \leftrightarrow (A - LC)^T P + P(A - LC) + (\gamma_1 + \gamma_2\gamma_3)I \\ &\quad + (\gamma_1 + \gamma_2\gamma_3\|b\|)PP < 0 \end{aligned} \tag{17}$$

The observer design (14) which has value of L, chosen such that the linear matrix inequality (17) is satisfied, has been proved in [27].

IV. APPLICATIONS OF LIPSCHITZ AND ADAPTIVE LIPSCHITZ OBSERVER DESIGNS TO THE MAMMALIAN MODEL

4.1 Mean value theorem

Lipschitz constants can be computed by using (3) or (4). However, these computations are sometimes difficult. In such cases, we can calculate Lipschitz constants by using the mean value theorem, which is described by

$$|f'(\zeta)| = \left|\frac{f(x) - f(\hat{x})}{x - \hat{x}}\right|, \tag{18}$$

where $\zeta \in [x, \hat{x}]$. The value of the Lipschitz constant is equivalent to the maximum value of function $f'(\zeta)$.

4.2 Choice of output values

Outputs of the mathematical model of mammalian circadian rhythms are not clearly specified in biology. Thus, in this paper, we manually select the outputs for the mammalian model. In order to use observers, the observability has to be guaranteed, that is, matrix (C, A) is observable. This condition is the prior condition in choosing the outputs of the mammalian model. Oscillations of circadian rhythms are mainly described by oscillations of proteins leading to the required measurements of the dynamics of the proteins. In other words, oscillations of mRNAs are less important than oscillations of proteins. Thus, the measurements of mRNAs may be reduced. Furthermore, since observers are designed for circadian models in order to show the possibility of reducing measurements, value of C should also be kept as simple as possible.

Based on the requirements just described, we choose the outputs for the mammalian model. A set of values C are chosen such that matrix (C, A) is observable. Among the selective set of values of C, we then choose values of C which have measurements of mRNAs reduced. However, since x_1, dynamic of *Per2*/*Cry* mRNA, will be used for the computation of Lipschitz constant of nonlinear function $\varphi_2(x_1)$ in mammalian model, its value has to be measurable. Besides x_1, values of x_3 and x_7 are also used to obtain Lipschitz constants of nonlinear functions $\varphi_1(x_3, x_7)$ and $\varphi_3(x_3)$. Therefore, these values have to be measurable. Given that the value of C is kept as simple as possible,

$$C = \begin{bmatrix} 1 & 0 & 0 & 0 & 0 & 0 & 0 \\ 0 & 0 & 1 & 0 & 0 & 0 & 0 \\ 0 & 0 & 0 & 0 & 0 & 0 & 1 \end{bmatrix}$$

can be chosen as the outputs of the mammalian model (1).

4.3 Application of Lipschitz observer design to the mammalian model

The mammalian model (1) can be expressed in the form of (2). Referring to (2), nonlinear functions $\varphi(x, u)$ of the mammalian model are obtained as

$$\varphi(x, u) = \begin{bmatrix} \varphi_1(x_3, x_7) \\ \varphi_2(x_1) \\ \varphi_3(x_3) \end{bmatrix} = \begin{bmatrix} \dfrac{v_{1b}(x_7 + c)}{k_{1b}\left(1 + \dfrac{x_3^p}{k_{ii}^p}\right) + x_7 + c} \\ x_1^q \\ \dfrac{v_{4b}x_3^r}{k_{4b}^r + x_3^r} \end{bmatrix}$$

Let γ_1, γ_2, and γ_3 be Lipschitz constants of $\varphi_1(x_3, x_7)$, $\varphi_2(x_1)$, and $\varphi_3(x_3)$ respectively. Lipschitz constant γ_2 is calculated first. According to (18),

$$|f'(\zeta_2)| = \left|q\zeta_2^{q-1}\right| = \left|\frac{\varphi_2(x_1) - \varphi_2(\hat{x}_1)}{x_1 - \hat{x}_1}\right|, \tag{19}$$

© 2013 Chinese Automatic Control Society and Wiley Publishing Asia Pty Ltd

where $\zeta_2 \in [\min(x_1, \hat{x}_1), \max(x_1, \hat{x}_1)]$. State x_1 is known and the oscillation of $x_1 \in [0, 1.518]$. We consider the oscilation of $\hat{x}_1 \in [0, 3.036]$. Therefore, $\zeta_2 \in [0, 3.036]$. With $q = 2$, the Lipschitz constant of $\varphi_2(x_1)$ is calculated as $\gamma_2 = 2 * |\zeta_2| = 6.072$.

It is difficult to obtain the Lipschitz constant γ_3 of $\varphi_3(x_3)$ directly from (3). Thus, equation (18) is used instead. According to (18),

$$|f'(\zeta_3)| = \left| -\frac{r v_{4b} k_{4b}^r \zeta_3^{r-1}}{(k_{4b}^r + \zeta_3^r)^2} \right| = \left| \frac{\varphi_3(x_3) - \varphi_3(\hat{x}_3)}{x_3 - \hat{x}_3} \right|, \tag{20}$$

where $\zeta_3 \in [\min(x_3, \hat{x}_3), \max(x_3, \hat{x}_3)]$. The maximum value of $|f'(\zeta_3)|$ is equivalent to Lipschitz constant γ_3, and this value is calculated by solving $|f''(\zeta_3)| = 0$. From Fig. 1, the dynamic of state variable $x_3 \in [0, 1.861]$. $\hat{x}_3$ is unknown. By considering $\hat{x}_3 \in [0, 3.722]$, we then obtain $\gamma_3 = 0.864$.

According to (3),

$$\|\varphi_1(x_3, x_7) - \varphi_1(\hat{x}_3, \hat{x}_7)\| \le \gamma_1 \left\| \begin{matrix} x_3 - \hat{x}_3 \\ x_7 - \hat{x}_7 \end{matrix} \right\|, \tag{21}$$

where γ_1 is Lipschitz constant. On the other hand, we have

$$\begin{aligned} &|\varphi_1(x_3, x_7) - \varphi_1(\hat{x}_3, x_7) + \varphi_1(x_3, x_7) - \varphi_1(x_3, \hat{x}_7)| \\ &\quad = |f'(\zeta_{1a})(x_3 - \hat{x}_3) + f'(\zeta_{1b})(x_7 - \hat{x}_7)| \end{aligned} \tag{22}$$

because according to (18),

$$|\varphi_1(x_3, x_7) - \varphi_1(\hat{x}_3, x_7)| = |f'(\zeta_{1a})||x_3 - \hat{x}_3|$$

$$|\varphi_1(x_3, x_7) - \varphi_1(x_3, \hat{x}_7)| = |f'(\zeta_{1b})||x_7 - \hat{x}_7|$$

where $\zeta_{1a} \in [\min(x_3, \hat{x}_3), \max(x_3, \hat{x}_3)]$ and $\zeta_{1b} \in [\min(x_7, \hat{x}_7), \max(x_7, \hat{x}_7)]$. Function $f'(\zeta_{1a})$ is the differentiated function of $\varphi_1(x_3, x_7)$ with respect to x_3, and function $f'(\zeta_{1b})$ is the differentiated function of $\varphi_1(x_3, x_7)$ with respect to x_7. Besides,

$$(22) \le \left\| \begin{matrix} f'(\zeta_{1a}) \\ f'(\zeta_{1b}) \end{matrix} \right\| \left\| \begin{matrix} x_3 - \hat{x}_3 \\ x_7 - \hat{x}_7 \end{matrix} \right\| \tag{23}$$

Therefore, inequality (21) is equivalent to inequality (23), and $\gamma_1 = \sqrt{(\max(f'(\zeta_{1a})))^2 + (\max(f'(\zeta_{1b})))^2}$. Maximum values of $f'(\zeta_2)$ and $f'(\zeta_3)$ are obtained by solving $|f''(\zeta_{1a})| = 0$ and $|f''(\zeta_{1b})| = 0$. In order to do this, values of states x_3 and x_7 and their estimates are required. From the value of C selected, the dynamics of states x_1, x_3, and x_7 are known. According to Fig. 1, the dynamics of states $x_3 \in [0, 1.861]$, $x_7 \in [0, 1.11]$. State estimates $\hat{x}_3$ and $\hat{x}_7$ are unknown. We chose $\hat{x}_3 \in [0, 3.722]$ for the case of $\varphi_3(x_3)$ above. For $\hat{x}_7$, we consider $\hat{x}_7 \in [0, 2.22]$. As a result, $\zeta_{1a} \in [0, 3.722]$ and $\zeta_{1b} \in [0, 2.22]$. These values are then substituted to solve $|f''(\zeta_{1a})| = 0$, and $|f''(\zeta_{1b})| = 0$. The results are obtained with $max(f'(\zeta_{1a})) = 1.9331 \times 10^{-15}$ and $max(f'(\zeta_{1b})) = 9$. As a result, $\gamma_1 = \sqrt{(1.9331 \times 10^{-15})^2 + (9)^2} = 9$.

Remark 2. [0, 3.036], [0, 3.722], and [0, 2.22], which are double the oscillation ranges of x_1, x_3, and x_7, are the possible ranges which we have chosen for the oscillation of $\hat{x}_1$, $\hat{x}_3$, and $\hat{x}_7$, respectively. Since $\hat{x}_1$, $\hat{x}_3$, and $\hat{x}_7$ are unknown, the ranges can be chosen differently. Nevertheless, in this paper, we consider [0, 3.036], [0, 3.722], and [0, 2.22] are the best performances for the chosen Lipschitz observer design, larger than which, the observer has a lack of efficiency.

Based on the three values of Lipschitz constants just computed, we then solve (8) by using the LMI toolbox in MATLAB. Results are obtained as

$$\sigma = 415.3313, L = \begin{bmatrix} 0.4004 & 0 & 0 \\ 0 & -0.0076 & 0 \\ 0 & 0.4242 & 0 \\ 0 & 0 & 0.0140 \\ 0 & 0 & 0.0064 \\ 0 & 0 & -0.0103 \\ 0 & 0 & 0.4144 \end{bmatrix}.$$

Error dynamics between the unmeasured states x_2, x_4, x_5, x_6, and their estimates are shown in Fig. 2, Fig. 3, Fig. 4, and Fig. 5.

Remark 3. The calculation of Lipschitz constants requires a region of oscillations of state variables. Each living species has its own circadian rhythms which are limit cycles. Thus, state variables of the mammalian model (1) are expected to have their known ranges of oscillations. Therefore, the

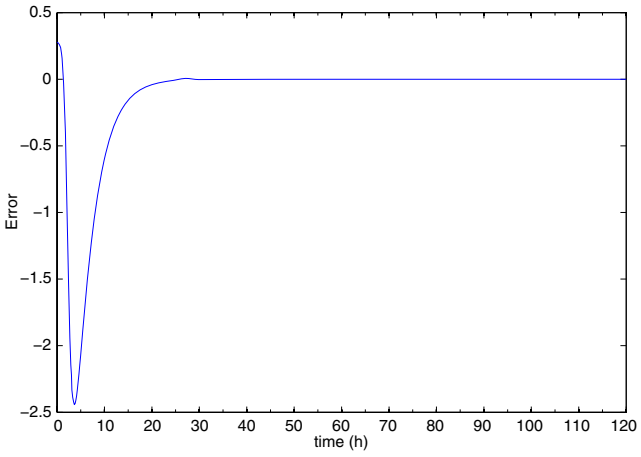

Fig. 2. Error between *Per*2/*Cry* mRNA and its estimate.

© 2013 Chinese Automatic Control Society and Wiley Publishing Asia Pty Ltd

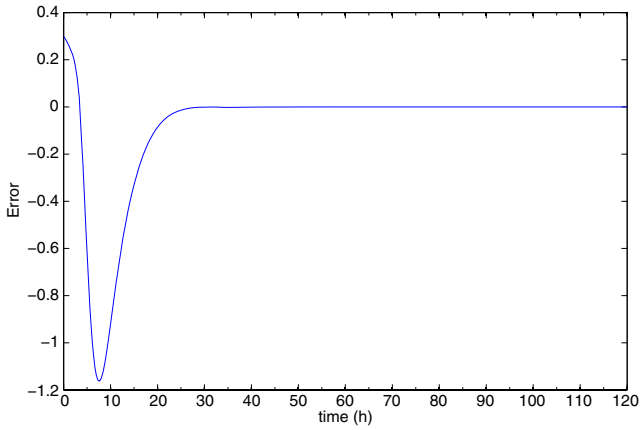

Fig. 3. Error between *Bmal*1 mRNA and its estimate.

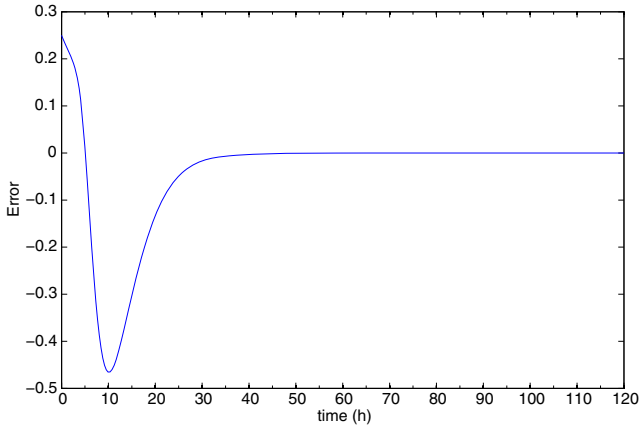

Fig. 4. Error between BMAL1 protein and its estimate.

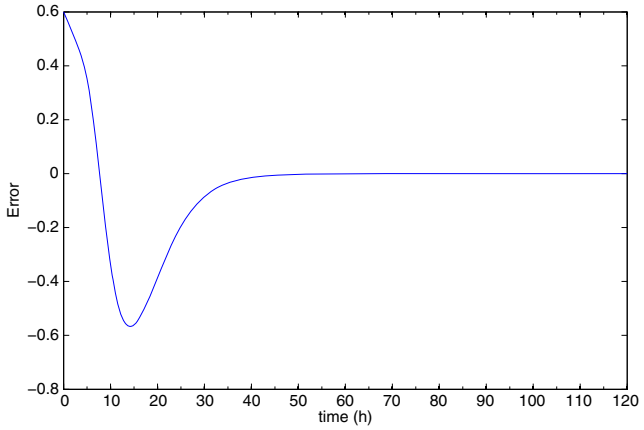

Fig. 5. Error between nuclear BMAL1 protein and its estimate.

calculation of Lipschitz constants for the observer of the mammalian model (1) can be carried out based on these ranges.

4.4 Application of adaptive Lipschitz observer design to mammalian model

In this section, the mammalian model (1) is considered to have unknown parameters. We choose parameter v_{1b} which represents the transcription rate of *Per2* mRNA as an unknown parameter. In research studies of mammalian rhythms, *Per2* is one of the genes which are responsible for the robustness to external environmental changes (*e.g.* light), and the transcription rate of *Per2* mRNA is regulated by light impulse [26]. Since the transcription rate of *Per2* mRNA (v_{1b}) is easily changed with light induced, v_{1b} is considered as an unknown parameter. The adaptive Lipschitz observer design is applied to the mammalian model in this case.

Rearranging system (1) to the form of system (9), the required parameters of the mammalian model are obtained as

$$\phi(x,u)=\begin{bmatrix}0\\ x_1^q\\ 0\\ \dfrac{v_{4b}x_3^r}{k_{4b}^r+x_3^r}\\ 0\\ 0\\ 0\end{bmatrix}, b=\begin{bmatrix}1\\0\\0\\0\\0\\0\\0\end{bmatrix}, \theta=v_{1b},$$

and

$$\varphi(x,u)=\begin{bmatrix}\dfrac{(x_7+c)}{k_{1b}\left(1+\dfrac{x_3^p}{k_{1i}^p}\right)+x_7+c}\end{bmatrix}$$

Computations of Lipschitz constants of each nonlinear function involved in $\varphi(x,\ u)$ and $\phi(x,\ u)$ have been carried out in the previous section. By using the values of these Lipschitz nonlinearities, we obtain Lipschitz constants of $\phi(x,\ u)$ and $\varphi(x,\ u)$ as $\gamma_1=\sqrt{(6.0720)^2+(0.8640)^2}=6.1332$ and $\gamma_2=9$ respectively. Since $v_{1b}=9$ is set as a default value of v_{1b}, and v_{1b} is considered as an unknown parameter, we may choose the value of γ_3 in $\|\theta\|\le\gamma_3$ as $\gamma_3=9$. The LMI toolbox in MATLAB is then used to solve (16). The results are obtained as $\sigma=15078$,

© 2013 Chinese Automatic Control Society and Wiley Publishing Asia Pty Ltd

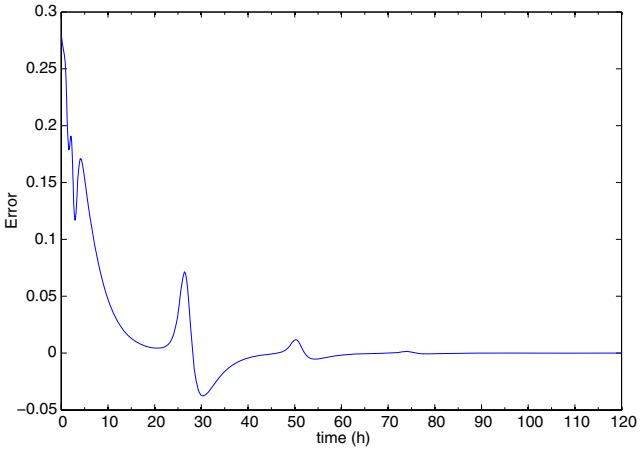

Fig. 6. Error between *Per2*/*Cry* mRNA and its estimate at $\rho = 50$.

$$P = \begin{bmatrix} 17329 & 0 & 0 & 0 & 0 & 0 & 0 \\ 0 & 23290 & 565 & 0 & 0 & 0 & 0 \\ 0 & 565 & 15169 & 0 & 0 & 0 & 0 \\ 0 & 0 & 0 & 14998 & 3969 & 1945 & -167 \\ 0 & 0 & 0 & 3969 & 24129 & 8156 & -117 \\ 0 & 0 & 0 & 1945 & 8156 & 20533 & -1733 \\ 0 & 0 & 0 & -167 & -117 & -1733 & 16653 \end{bmatrix},$$

$$L = \begin{bmatrix} 0.4351 & 0 & 0 \\ 0 & -0.0121 & 0 \\ 0 & 0.4974 & 0 \\ 0 & 0 & -0.0023 \\ 0 & 0 & 0.0109 \\ 0 & 0 & 0.0345 \\ 0 & 0 & 0.4571 \end{bmatrix}.$$

It can be verified that $b^T P C^{\perp} = 0$. The adaptive gain $\rho = 50$ is set. Error dynamics of the unmeasured states x_2, x_4, x_5, x_6, and their estimates are shown in Fig. 6, Fig. 7, Fig. 8, and Fig. 9, respectively. Estimation of the unknown parameter v_{1b} is shown in Fig. 10.

Remark 4. In the mechanism of mammalian model (1), BMAL1* protein will activate the production of the *Per2* mRNA and *Cry* mRNA seperately. Then these two mRNAs will be phosphorylated to form *Per2*/*Cry* mRNA. v_{1b} represents the amount of *Per2* mRNA and *Cry* mRNA produced in an hour after the impact of BMAL1* protein. As easily influenced by light, this parameter is hard to measure. Thus, it is considered as an unknown parameter in this paper.

Remark 5. Besides the transcription rate of *Per2*/*Cry* mRNA v_{1b}, there are other parameters which could be considered as unknown parameters based on the parametric sensitivity analysis in [29]. The adaptive Lipschitz observer design described in this paper can also work with these unknown parameters.

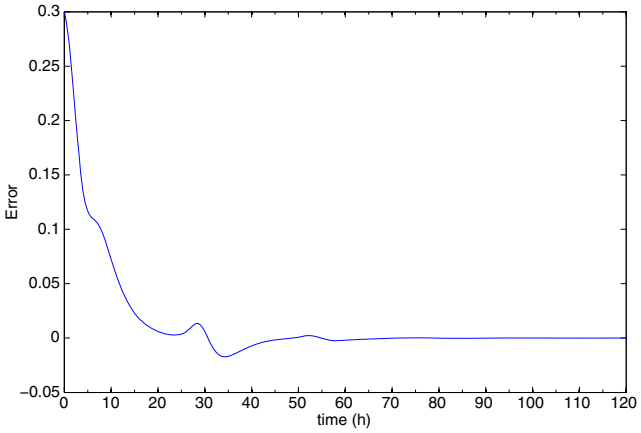

Fig. 7. Error between *Bmal*1 mRNA and its estimate at $\rho = 50$.

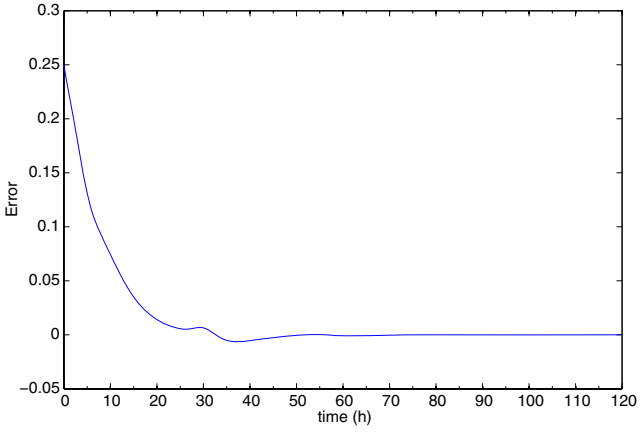

Fig. 8. Error between BMAL1 protein and its estimate at $\rho = 50$.

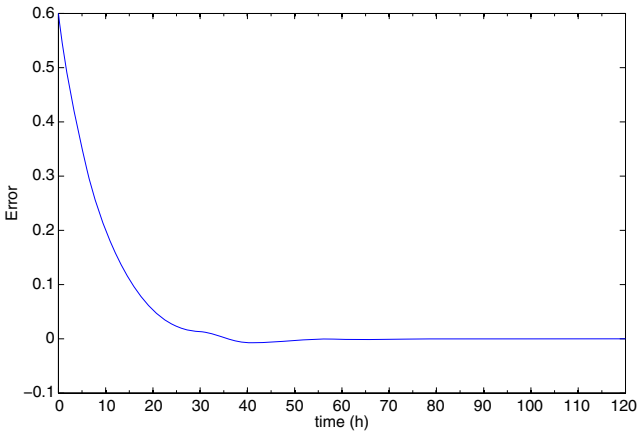

Fig. 9. Error between nuclear BMAL1 protein and its estimate at $\rho = 50$.

© 2013 Chinese Automatic Control Society and Wiley Publishing Asia Pty Ltd

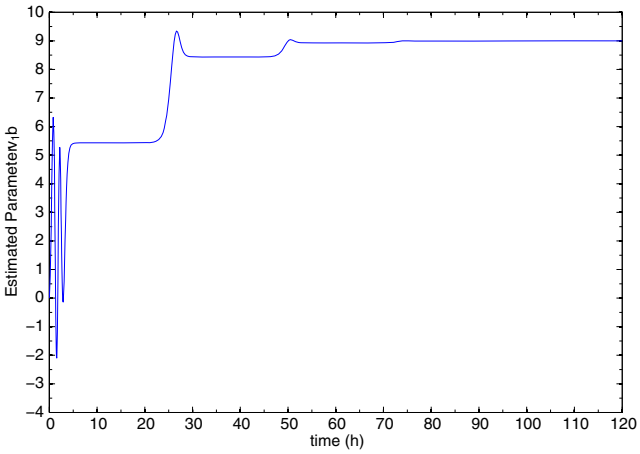

Fig. 10. Estimate of parameter v_{1b} at $\rho = 50$.

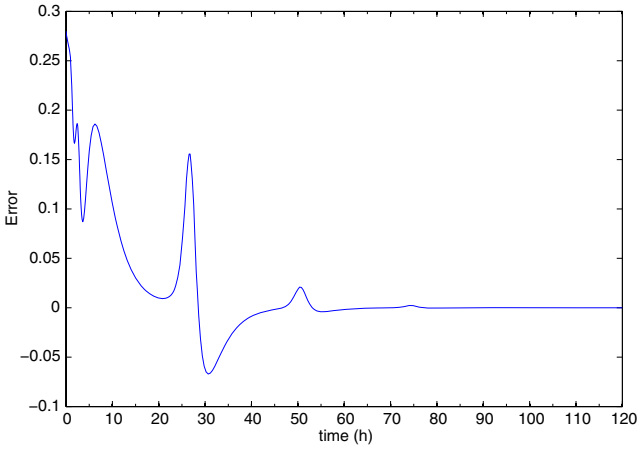

Fig. 11. Error between *Per*2/*Cry* mRNA and its estimate at $\rho = 70$.

4.5 Discussion

Since there are a lack of applications of observer designs to circadian models, the result obtained in [25] is used to judge the performances of both proposed Lipschitz observer designs. According to [25], with control of light input, the phase is restored and tracked within 40 h. Therefore, we expect the desired performances of both Lipchitz observer designs given in Section III are also within 40 h ($0h \leq \tau \leq 40h$). Fig. 2 to Fig. 5 have shown that the performances of the Lipschitz observer applied to the mammalian model are within the desired range of time. Meanwhile, the results obtained in Fig. 6 to Fig. 9 have shown that the adaptive Lipschitz observer does not satisfy the desired performances. The proposed adaptive observer design takes a longer time to estimate the unknown states. This is affected by the slow convergence rate of estimation of unknown parameter which is shown in Fig. 10.

Variations in value of the adaptive gain ρ can change the performance of the adaptive Lipschitz observer. Value of ρ is reset as $\rho = 70$. Error dynamic between the unmeasured state x_2 and its estimate is shown in Fig. 11. The result depicted in Fig. 11 shows that estimate of state variable x_2 converges to its actual value at approximately $t_1 = 63h$. Since $t_1 > 40h$, the performance of the adaptive Lipschitz observer is not within the desired range of time.

Remark 6. The estimations of unknown parameter v_{1b} at $\rho = 70$ and $\rho = 10$ are shown in Fig. 12 and Fig. 14 respectively.

The value of ρ is then adjusted to $\rho = 10$. In this case, the error dynamic between the unmeasured state x_2 and its estimate is shown in Fig. 13. According to Fig. 13, the unknown state x_2 is successfully estimated at approximately

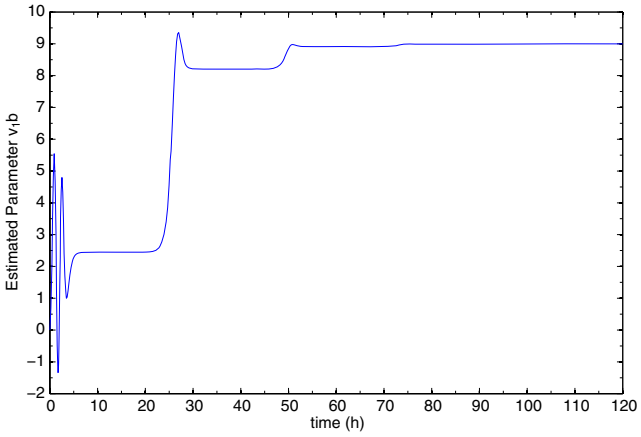

Fig. 12. Estimate of parameter v_{1b} at $\rho = 70$.

$t_2 = 35h$. Since $t_2 < 40h$, the proposed adaptive Lipschitz observer design has its performances satisfied. However, because of the large density of transient oscillations occuring in the dynamic of the estimate of the unknown parameter v_{1b} (shown in Fig. 14), the performances achieved at $\rho = 10$ are not ideal performances. Thus, $\rho = 10$ is not the ideal value for ρ.

For values of $\rho < 50$, density of transient oscillations is increased in the estimation of the unknown parameter. For values of $\rho > 50$, the adaptive Lipschitz observer takes a longer time to estimate either the unknown state variables or the unknown parameter. Therefore, $\rho = 50$ is considered as the ideal value of ρ. Although the performance of the adaptive Lipschitz observer at $\rho = 50$ is not within the desired range of time, it is still acceptable if it is compared with the performance achieved in practice, where the dynamics of state variables of the mammalian model (1) may require a large amount of time (about 3–4 days) to be tracked.

© 2013 Chinese Automatic Control Society and Wiley Publishing Asia Pty Ltd

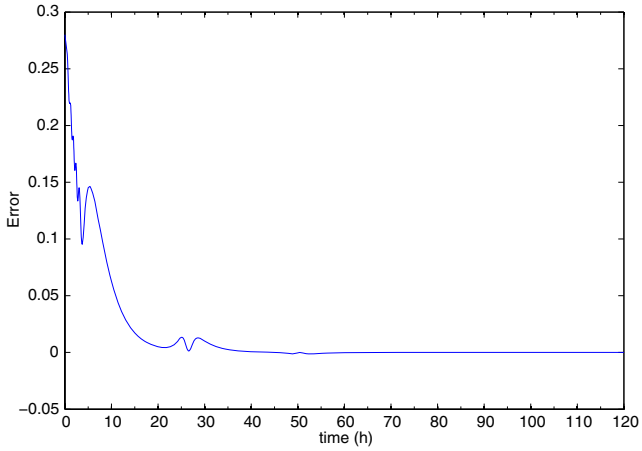

Fig. 13. Error between *Per*2/*Cry* mRNA and its estimate at $\rho = 10$.

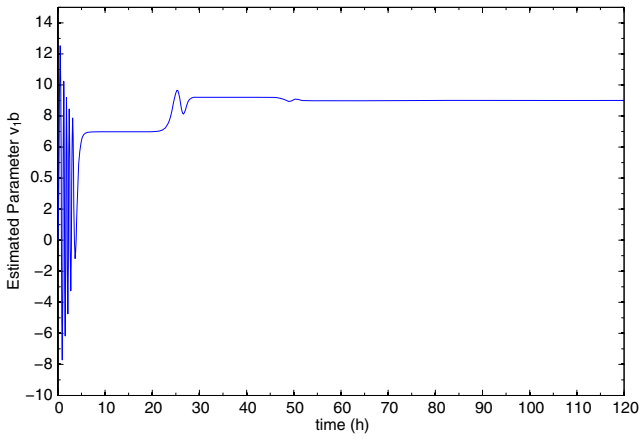

Fig. 14. Estimate of parameter v_{1b} at $\rho = 10$.

V. CONCLUSIONS

We have analyzed the nonlinearities in a circadian model of Mammals, and have shown that observers with Lipschitz nonlinearities can be applied. The performances of two observer designs, Lipschitz and adaptive Lipschitz, have been evaluated by simulation studies. Detailed evaluation does show that both proposed observers give asymptotic estimates of unmeasured state variables. The convergence rate of the adaptive Lipschitz observer design depends on the speed of estimation of the unknown parameter. Changes in value of the adaptive gain can affect the convergence rate of the unknown parameter.

For circadian models having high order and strong nonlinearities, the measurements of the internal state variables of these models are sometimes either difficult for direct calculation or time-consuming. With a reduction of measurements, we may avoid these problems. As shown in the above results, with only three known state variables, we have been able to estimate the remaining state variables of the 7th order mammalian model. Therefore, besides the successful application of observer to the mammalian model, we have also shown a possibility of reducing measurements in the biological study of circadian rhythms.

REFERENCES

1. Leloup, J. C. and A. Goldbeter, "Modelling the dual role of Per phosphorylation and its effect on the period and phase of the mammalian circadian clock," *IET Syst. Biol*, Vol. 5, pp. 44–49 (2011).
2. Li, Y., Z. Liu, J. Zhang, R. Wang, and L. Chen, "Synchronization mechanisms of circadian rhythms in the suprachiasmatic nucleus," *IET Syst. Biol*, Vol. 3, pp. 100–112 (2009).
3. Dong, W., X. Tang, Y. Yu, J. Griffith, R. Nilsen, D. Choi, J. Baldwin, L. Hilton, K. Kelps, J. Mcguire, R. Morgan, M. Smith, M. Case, J. Arnold, H. B. Schttler, Q. Wang, J. Liu, J. Reeves, and D. Logan, "Systems biology of the Neurospora biological clock," *IET Syst. Biol*, Vol. 1, pp. 257–265 (2007).
4. Bunger, M. K., L. D. Wilsbacher, S. M. Moran, C. Clendenin, L. A. Radcliffe, J. B. Hogenesch, M. C. Simon, J. S. Takahashi, and C. A. Bradfield, "Mop3 is an Essential Component of the Master Circadian Pacemaker in Mammals," *Cell*, Vol. 103, pp. 1009–1017 (2000).
5. Horst, G. T. J. V. D., M. Muijtjens, K. Kobayashi, R. Takano, S. Kanno, M. Takao, J. de Wit, A. Verkerk, A. P. Eker, D. van Leenen, R. Buijs, D. Bootsma, J. H. Hoeijmakers, and A. Yasui, "Mammalian Cry1 and Cry2 are essential for maintenance of circadian rhythms," *Nature*, Vol. 398, pp. 627–630 (1999).
6. Bae, K., X. Jin, E. S. Maywood, M. H. Hastings, S. M. Reppert, and D. R. Weaver, "Differential Functions of mPer1, mPer2, and mPer3 in the SCN Circadian Clock," *Neuron*, Vol. 30, pp. 525–536 (2001).
7. Takahashi, J. S., M. H. Vitaterna, D. P. King, A. M. Chang, J. M. Kornhauser, P. L. Lowrey, J. D. McDonald, W. F. Dove, L. H. Pinto, and F. W. Turek, "Mutagenesis and mapping of a mouse gene, Clock, essential for circadian behaviour," *Science*, Vol. 264, pp. 719–725 (1994).
8. Gonze, D., J. C. Leloup, and A. Goldbeter, "Theoretical models for circadian rhythms in Neurospora and Drosophila," *Comptes Rendus de l'Acadmie des Sciences—Series III—Sciences de la Vie*, Vol. 323, pp. 57–67 (2000).
9. Francose, P., "A model for the neurospora circadian clock," *Biophys. J.*, Vol. 88, pp. 2369–2383 (2005).
10. Goldbeter, A., "A model for circadian oscillations in the Drosophila period protein (PER)," *Proc. Biol Sci.*, Vol. 261, pp. 319–324 (1995).

© 2013 Chinese Automatic Control Society and Wiley Publishing Asia Pty Ltd

11. Weimann, S. B., J. Wolf, H. Herzel, and A. Kramer, "Modelling feedback Loops of the Mammalian Circadian Oscillator," *Biophys. J.*, Vol. 87, pp. 3023–3034 (2004).
12. Kurosawa, G. and A. Goldbeter, "Amplitude of circadian oscillations entrained by 24-h light-dark cycles," *J. Theor. Biol.*, Vol. 242, pp. 478–488 (2006).
13. Geier, F., S. Becker-Weimann, A. Kramer, and H. Herzel, "Entrainment in a model of the mammalian circadian oscillator," *J. Biol. Rhythms*, Vol. 20, pp. 83–176 (2005).
14. Stelling, J., E. D. Gilles, and F. J. Doyle III, "Robustness properties of circadian clock architectures," *Proc. Natl Acad Sci. USA*, Vol. 101, pp. 13210–13215 (2004).
15. Gunawan, R. and F. J. Doyle III, "Isochron-Based Phase Response Analysis of Circadian Rhythms," *Biophys. J.*, Vol. 91, pp. 2131–2141 (2006).
16. Gunawan, R., S. R. Taylor, L. R. Petzold, and F. J. Doyle III, "Sensitivity Measures for Oscillating Systems: Application to Mammalian Circadian Gene Network," *IEEE Trans. Autom. Control*, Vol. 53, pp. 177–188 (2008).
17. Fey, D., R. Findeisen, and E. Bullinger, "Parameter estimation in kinetic reaction models using nonlinear observers facilitated by model extensions," *17th IFAC World Congress*, Seoul, Korea, pp. 313–318 (2008).
18. Ding, Z., "Global Output Feedback Stabilization of Nonlinear Systems with nonlinearity of Unmeasured States," *IEEE Trans. Autom. Control*, Vol. 54, pp. 1117–1122 (2009).
19. Ding, Z., "Differential stability and design of reduced order observers for nonlinear systems," *IET Control Theory Appl.*, Vol. 5, pp. 315–322 (2011).
20. Zhao, Y., J. Tao, and N. Z. Shi, "A note on observer design for one-sided Lipschitz nonlinear systems," *Syst. Control Lett.*, Vol. 59, pp. 66–71 (2010).
21. Maywood, E. S., J. A. O'Brien, and M. H. Hastings, "Expression of mCLOCK and other circadian clock-relevant proteins in the mouse suprachiasmatic nuclei," *J. Neuroendocrinol.*, Vol. 15, pp. 329–334 (2003).
22. Eide, E. J., E. L. Vielhaber, W. A. Hinz, and D. M. Virshup, "The circadian regulatory proteins BMAL1 and cryptochromes are substrates of casein kinase Iepsilon," *J. Biol. Chem.*, Vol. 277, pp. 17248–17254 (2002).
23. Nicholas, G., S. David, B. N. Hubert, C. D. Fred, D. W. Lisa, P. K. David, S. T. Joseph, and J. W. Charles, "Role of the CLOCK protein in the mammalian circadian mechanism," *Science*, Vol. 280, pp. 1564–1569 (1998).
24. Hu, G. D., "Observers for one-sided Lipschitz nonlinear systems," *IMA J. Math. Control Inf.*, Vol. 23, pp. 395–401 (2006).
25. Shaik, O. S., S. Sager, O. Slaby, and D. Lebiedz, "Phase tracking and restoration of circadian rhythms by model-based optimal control," *IET Syst. Biol.*, Vol. 2, pp. 16–23 (2008).
26. Caldelas, I., V. J. Poirel, B. Sicard, P. Pévet, and E. Challet, "Circadian profile and photic regulation of clock genes in the suprachiasmatic nucleus of a diurnal mammal Arvicanthis ansorgei," *Neuroscience*, Vol. 116, pp. 583–591 (2003).
27. Cho, Y. M. and R. Rajamani, "A Systematic Approach to Adaptive Observer Synthesis for Nonlinear Systems," *IEEE Trans. Autom. Control*, Vol. 42, pp. 534–537 (1997).
28. TonThat, L. and Z. Ding, "One-sided Lipschitz observer design for circadian models," *50th IEEE Conference on Decision and Control and European Control Conference (CDC-ECC)*, Orlando, FL, pp. 71–76 (2011).
29. Bagheri, N., J. Stelling, and F. J. Doyle III, "Circadian Phase Resetting via Single and Multiple Control Targets," *PLoS Computational Biology*, Vol. 4 (2008).

Long Ton That was born in 1985 in Vietnam. After the merger of University of Manchester (UK) and University of Manchester Institute of Science and Technology (UMIST), he received his B.Eng. degree in 2007, M.Sc. and Ph.D. degrees in 2008 and 2012 respectively.

Zhengtao Ding was born in 1964 in Jiangsu, China. He obtained his B.Eng. degree from Tsinghua University, Beijing, in 1984, M.Sc. and Ph.D. degrees in 1986 and 1989 respectively from Control Systems Centre, University of Manchester Institute of Science and Technology (UMIST), UK. Having worked in UK universities as a research fellow for a few years, he joined Ngee Ann Polytechnic, Singapore, in 1993, as a lecturer in Department of Mechanical Engineering. Since September 2003, he has been a lecturer and then senior lecturer in control engineering with University of Manchester in Control Systems Centre, School of Electrical and Electronic Engineering. Dr. Ding's main research interest is in control theory and applications, in particular, adaptive and robust control of uncertain nonlinear systems, consensus control, disturbance rejection and output regulation.

© 2013 Chinese Automatic Control Society and Wiley Publishing Asia Pty Ltd